Kaon Production Target for Hall D at Jefferson Laboratory (Technical Note)

Igor Strakovsky,[1,*] Moskov Amaryan,[2] Mikhail Bashkanov,[3] Vitaly Baturin,[4] William J. Briscoe,[1] Eugene Chudakov,[5] Pavel Degtiarenko,[5] Sean Dobbs,[6] Hovanes Egiyan,[5] Alexander Laptev,[7] Ilya Larin,[8] Alexander Somov,[5] and Timothy Whitlatch[5]

[1] *The George Washington University, Washington, DC 20052, USA*
[2] *Old Dominion University, Norfolk, VA 23529, USA*
[3] *University of York, Heslington, York YO10 5DD, UK*
[4] *Old Dominion University, Norfolk, VA 20529, USA*
[5] *Thomas Jefferson National Accelerator Facility, Newport News, VA 23606, USA*
[6] *Florida State University, Tallahassee, FL 32306, USA*
[7] *Los Alamos National Laboratory, Los Alamos, NM 87545, USA*
[8] *University of Massachusetts, Amherst, MA 01003, USA*

(Dated: July 21, 2023)

The Kaon Production Target (KPT) is an important component of the proposed K-Long Facility (KLF) for strange hadron spectroscopy in Hall D at JLab [1]. In this note we present a conceptual design for the Be-target assembly for the planned K-Long beam line, which will be used along with the GlueX spectrometer in its standard configuration for the proposed experiment. The high intensity 12 GeV CEBAF electron beam with 5 μA current enables creation of intensive bremßtrahlung photon beam to produce the flux of K_L beam on the order of $\sim 10^4$ K_L/sec on the GlueX target exceeding the K_L flux previously obtained at SLAC by three orders of magnitude. The most important requirement for the KPT is to make sure that the neutron and the photon flux accompanying secondary K_L beam is well under control from radiation point of view. The Monte Carlo simulations for the proposed conceptual design of KPT show that the resulting neutron and gamma flux lead to a prompt radiation dose rate for the KLF experiment that is below the JLab Radiation Control Department radiation dose rate limits in the experimental hall and at the site boundary and will have no impact on the performance of the GlueX spectrometer.

CONTENTS

* Corresponding author; igor@gwu.edu

I. KLF PHYSICS CASE

The GlueX spectrometer in Hall D at Jefferson Lab, shown in Figure 1, is a powerful tool employed by the GlueX Collaboration to investigate a wide range of topics in meson and baryon spectroscopy and structure, particularly the search for mesons with excited gluonic content, using the recently upgraded 12 GeV electron beam of CEBAF accelerator. The spectrometer is carefully designed [2] to measure charged and neutral final state particles with almost 4π acceptance.

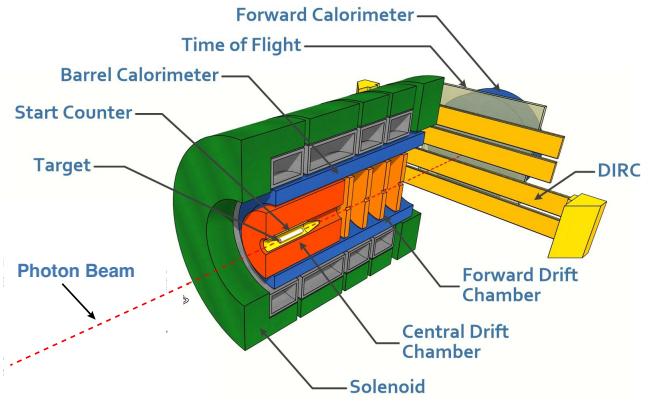

FIG. 1. The GlueX spectrometer.

The proposed secondary K_L beam at Jefferson Laboratory [1] will revolutionize our understanding of bound systems containing strange quarks by providing the long-sought, high quality experimental data required to reach deeper understanding of the role of strange quarks in hadrons. It is expected that this facility will enable significant new progress in the strange hadron spectroscopy, both in the experimental, as well as theoretical understanding of these states. It will also have a high impact on the experimental program of strange hadron spectroscopy using electromagnetic probes bringing them into a new frontier. The facility and its associated physics program would allow the hadron spectroscopy communities around the world to make an exciting new scientific advances. The existing infrastructure at Jefferson Lab is well suited to provide a new, world class kaon beam facility to enable groundbreaking progress in our field in the next decade. We are confident that obtained new experimental data will significantly enrich the physics program of the hadron spectroscopy in general and the scientific community at Jefferson Lab will continue its world leading standing in this field.

The study of the strange hadrons provides a natural motivation for the future measurements at Jefferson Lab well in accord with the long range plan summarized in **Reaching for the Horizon: Long Range Plan for Nuclear Science** [3]: *For many years, there were both theoretical and experimental reasons to believe that the strange sea-quarks might play a significant role in the nucleon's structure; a better understanding of the role of strange quarks became an important priority.*

We propose to create a secondary beam of neutral kaons in Hall D at Jefferson Lab to be used with the GlueX experimental setup for the strange hadron spectroscopy [1]. The superior CEBAF electron beam will enable a flux of neutral long-lived kaons on the order of $\sim 10^4$ K_L/sec, which exceeds the kaon flux previously attained at SLAC [8] by three orders of magnitude. The use of the deuterium target in addition to the standard liquid hydrogen target will provide the first ever measurements of the neutral kaons interacting with neutrons. The ability of the GlueX spectrometer to measure reaction fragments over the wide ranges of a polar θ and azimuthal ϕ angles with a good coverage for both a charged and a neutral particles (see, for instance, Refs. [9–11]), together with the K_L momentum information from the K_L time-of-flight, provides an ideal environment for these measurements.

Our KLF proposal *Strange hadron spectroscopy with secondary K_L beam in Hall D* C12–19–001 received a full approval from the PAC48 [4] to run in Hall D for 200 PAC days.

As a part of the KLF project, three new critical elements will be added to the Hall D beamline: the Compact Photon Source (CPS) [5], the Kaon Production Target (KPT) [6], and the Kaon Flux Monitor (KFM) [7].

In this work, we describe a conceptual design for the KPT that satisfies the requirements for the KLF program, and show through simulations that the expected radiation and heat deposition are within acceptable limits.

II. THE KLF BEAMLINE

A schematic view of the proposed Hall D beam line for the KLF project showing the production chain $e \to \gamma \to K_L$ is given in Fig. 2.

At the first stage, 12 GeV electrons with a 5 μA current scatter off of a copper radiator (10% X_0) contained inside the CPS [5] generating an intense beam of untagged bremßtrahlung photons, which then travels $\approx 65m$ towards the KPT. The energy spectrum of this photon beam that reaches the upstream end of the KPT Beryllium target is shown in Fig. 3, and has a total power of approximately 5.7 kW. The photon beam has an intensity at the KPT of 4.7×10^{12} γ/sec for $E_\gamma > 1.5$ GeV, which corresponds to the production threshold of the ϕ-meson, which is the main source of the K_L beam. The remaining power of the 12 GeV, 60 kW electron beam is deposited within the CPS assembly which also acts as an electron beam dump.

The CPS will be located downstream of the Hall-D tagger magnet. The existing Hall D tagger magnet and detectors will not be used.

At the second stage, the bremsstrahlung photons hit the Be target located at the upstream end of the collimator alcove of the main experimental hall (see Fig. 5)

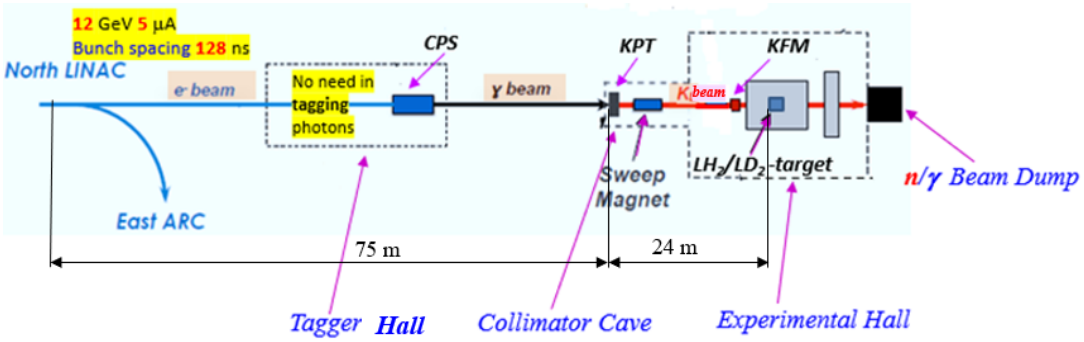

FIG. 2. Schematic view of the KLF beam line in Hall D with the production chain $e \to \gamma \to K_L$. The main components are the CPS, KPT, sweep magnet, and KFM (see text for details). The beam goes from the left to the right.

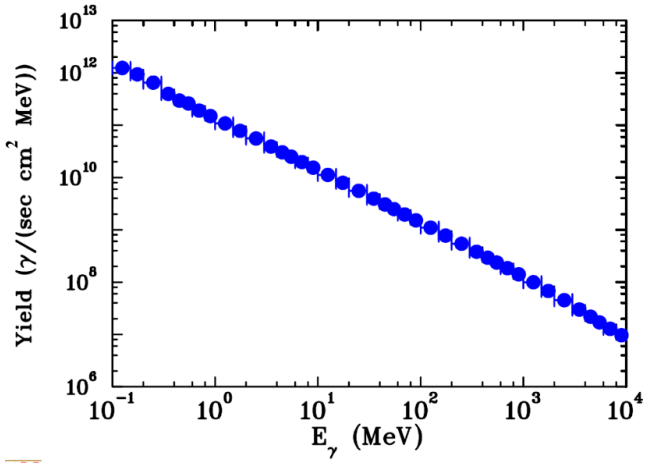

FIG. 3. fff03 The energy spectrum of the bremsstrahlung photons on the face of the Be-target. Calculations were performed using the MCNP radiation transport code [12].

and produce a beam containing neutral kaons with flux $\sim 10^4$ K_L/sec, neutrons with flux $\sim 6.6 \times 10^5$ n/sec, a smaller flux of photons, and charged particles. The charged particles are then removed from the beam with a sweep magnet, leaving a beam that is dominantly composed of neutral kaons and neutrons.

III. PROPOSED CONCEPT FOR THE BERYLLIUM TARGET

The KPT is built around a Beryllium target with 40 cm length and 6 cm diameter, and will be located in the collimator alcove in Hall D. This concept follows the successful use of beryllium targets for K_L production at SLAC [13] and NINA [14]. A schematic view of the Be-target assembly is given in Fig. 4. In this section, we describe the conceptual design of this target assembly and the expected secondary beam characteristics.

The collimator alcove has enough room to hold the additional shielding and beam line components required to prepare the K_L beam before it reaches the main part of the experimental hall. Since it is planned to be able to switch between the photon and K_L beam line configurations, we note that the collimator alcove is wide enough, at 4.52 m in width, for the Be target assembly to be moved to the side (Fig. 5) and remain far enough from the beam line to allow for the reinstallation of photon beam line components when Hall D switches to regular photon beam mode. Sufficient water cooling is also already available in this alcove to dissipate the approximately 5.3 kW of power delivered by the photon beam to the KPT assembly.

We have performed comprehensive simulations of the neutron, photon, and muon backgrounds to optimize the KPT design and to evaluate the resulting radiation levels and their possible influence on the performance of the GlueX detector. The most important and damaging background comes from neutrons. To estimate the neutron and gamma flux in the beam and the neutron prompt radiation dose rate in the experimental hall from scattered neutrons and gammas, we used the MCNP6 N-Particle (MCNP) radiation transport code [12].

For the MCNP calculations (in terms of flux [part/s/cm^2/MeV] or biological dose rate [mrem/h]), many tallies, *i.e.*, spots where we calculated the flux or dose rate, were placed along the beam and in the experimental hall and the alcove for the neutron and gamma fluence estimation. Fluence-to-Effective Dose conversion factors from ICRP 116 [15] were implemented to convert the neutron and gamma fluences into effective dose rates. We used the material composition data for the radiation transport modeling from Ref. [16].

The MCNP simulations are based on the advanced nuclear cross section libraries created and maintained by several DOE National Laboratories. The physical models implemented in the MCNP6 code take into account bremßtrahlung photon production, photo nuclear reactions, neutrons and photons multiple scattering processes. The experimental hall, collimator alcove, and the photon beam produced in CPS were modeled using the specifications from the layout presented in Figure 5, shown as a 3D graphic model of the experimental setup.

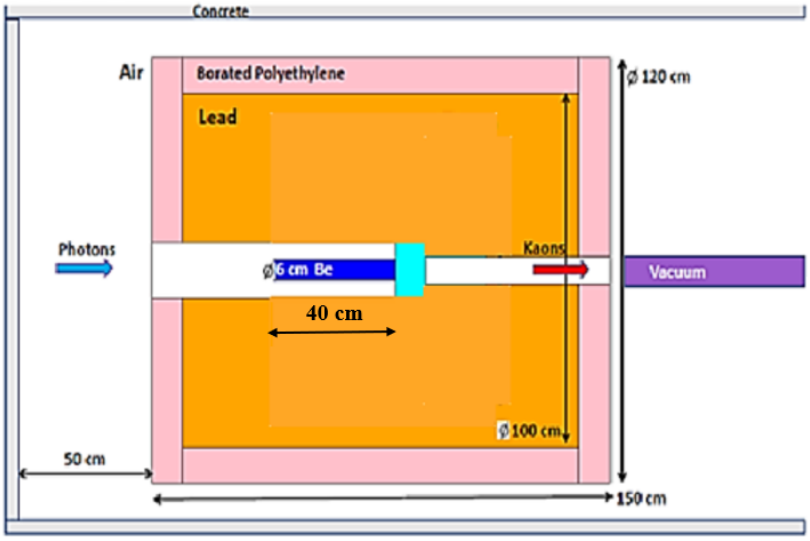

FIG. 4. fff06 Schematic view of the KPT assembly. Concrete, borated polyethylene, lead, tungsten, beryllium, vacuum beam pipe, and air shown by grey, pink, brown, light blue, blue, violet, and white colors, respectively. The beam goes from the left to the right.

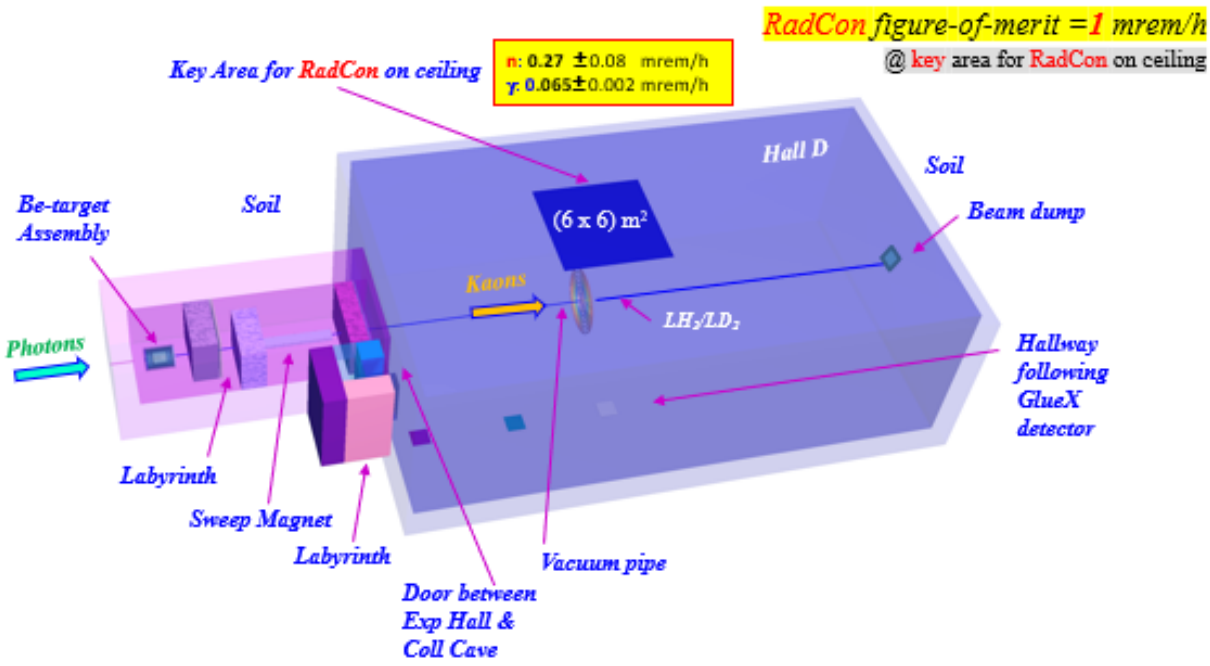

FIG. 5. fff04 Schematic view of Hall D setting for the MCNP radiation transport code [12] calculations. The model is presented as semi-transparent for demonstration purposes. The beam goes from the left to the right.

Additional radiation studies and calculations of power deposition were performed with the FLUKA (version FLUKA2021.2.9) software package [17].

A. Target and Plug Materials and Dimensions

The K_L beam will be produced through interactions of the photon beam with a beryllium target of 40 cm length and 6 cm diameter. The target is made of beryllium because the lighter elements have a higher photoproduction yield with a lower absorption of K_L's and a large radiation length, as pointed out in previous SLAC studies [21].

The length of the target was optimized by MC simulations of the K_L yield versus Be target length in a different ranges of K_L momenta shown in Fig. 6.

Other target materials, such as carbon, that would be easier to handle than beryllium were considered. However the simulations we performed show that a beryllium target performs significantly better than a similar target made of carbon. Namely, Pythia [18] simulations showed that the kaon yield from beryllium is a factor 1.51 larger than that from carbon at the same radiation length. From MCNP simulations, we also found that the absorption of neutrons in a beryllium target is about ~ 1.45 larger than in a similar carbon target. From both of these considerations, beryllium is the preferred target material. We performed Monte-Carlo simulations to optimize the length of the target by studying the K_L yield versus beryllium target length in different ranges of K_L momenta, as shown in Fig. 6. We also estimated that the rate of neutral kaons produced in the tungsten plug was negligible compared to the rate of kaons produced in the beryllium target. Based on these studies, we decided to use a 40 cm long beryllium target.

A tungsten beam plug of 10 cm thickness ($\sim$ 30 r.l.) and 15×15 cm^2 transverse size is attached to the downstream end of the beryllium target (as illustrated in Fig. 4) to clean up the beam and absorb induced radiation. In earlier studies at SLAC [21], it was shown that tungsten is an optimal material for the plug and that the tungsten has a lower absorption factor for kaons as compared to copper. We confirmed this effect through Pythia simulations, where we found the ratio of K_L's surviving after a tungsten beam plug to one made of copper to be 1.16 (1.36) for kaon momentum of 1 GeV/c (0.5 GeV/c). Using MCNP simulations, we also found that the tungsten plug more effectively reduces the flux of secondary neutrons and photons compared to lead or copper of the same length. The positive effect of tungsten material compared to lead (copper) was found to be 2.25 (9.29) times lower flux of neutrons and 8.11 (66.8) for photons. From these considerations, tungsten was chosen as the preferred beam plug material.

The yield of kaons from the tungsten plug was estimated to be negligible compared to the rate of kaons produced in the beryllium target. From these considerations, tungsten was chosen as the preferred beam plug material.

The dimensions of the tungsten plug were also optimized. It was found that increasing the plug diameter will increase the neutron background. For example, increasing the diameter to 24 cm from 16 cm yields an increase of neutron production by a factor of 2.8. This effect is due to re-scattered neutrons in the plug. However, there is no significant effect for photons.

It was also found that increasing the plug length will decrease the neutron and photon backgrounds. For example, increasing the plug length to 15 cm from 10 cm results factor of 0.6 for neutron production, and even a larger factor for photon production. However, increasing the plug length also reduces the number of K_L's which exit the KPT. Therefore, we take the final length to be 10 cm.

B. Location of the Be-target Assembly

To reduce the effect of the neutron and photon background coming from the beryllium target and tungsten plug into the experimental hall, we place the KPT upstream of the GlueX spectrometer in the collimator alcove (see Fig. 5). Additional shielding inside the collimator alcove is added to minimize the neutron and γ background in the experimental hall and to satisfy the JLab RadCon radiation dose rate limit in the experimental hall (1 mrem/h), which is roughly based on the requirement to limit the yearly dose accumulation at the CEBAF boundary at 10 mrem. The key area for the dose rate evaluation in the main experimental hall is in the area of (6×6) m^2 on the ceiling of the experimental hall centered above the GlueX detector, as shown in Fig. 5. The dose rate limit at that location roughly corresponds to the expected dose rate at the CEBAF fence at the level of 1 μrem/h, as both evaluated and observed at other locations at CEBAF (in the vicinity of the high power End Stations of Halls A and C). The Fig. 7 illustrates typical radiation dose rates currently observed around the Collimator Cave at Hall D during photon beam operation, which are generally $\lesssim 100$ mrad/h. The task for the shielding design of the Be target assembly in the Collimator Cave for the new experiment is to keep the radiation environment in the hall at or below the typical current level, both during and after beam delivery.

A vacuum beam pipe extends between the KPT and the cryogenic target, and prevents the beam kaons and background neutrons and photons re-scattering in the air in the experimental hall. Directly downstream of the Be target there will be a sweeping magnet with a field integral of 0.8 T $\cdot$ m to remove up the charged particle component from the beam.

C. The Kaon and Neutron Flux

Charged particles produced by the interaction of the photon beam with the KPT are removed by a sweep magnet downstream of the KPT. The resulting beam consists primarily of neutrons and K_L's, and in this section we calculate their properties. Neutral kaon production by bremßtrahlung photons was simulated using the PYTHIA MC generator [18]. The photon flux on the KPT face shown in Fig. 3 was used as input for Monte Carlo simulations. The main mechanism of K_L production in our energy range is via ϕ-meson photoproduction, which yields the same number of K^0 and $\overline{K}^0$.

The neutron flux calculations were performed using the MCNP radiation transport code [12], and a simplified

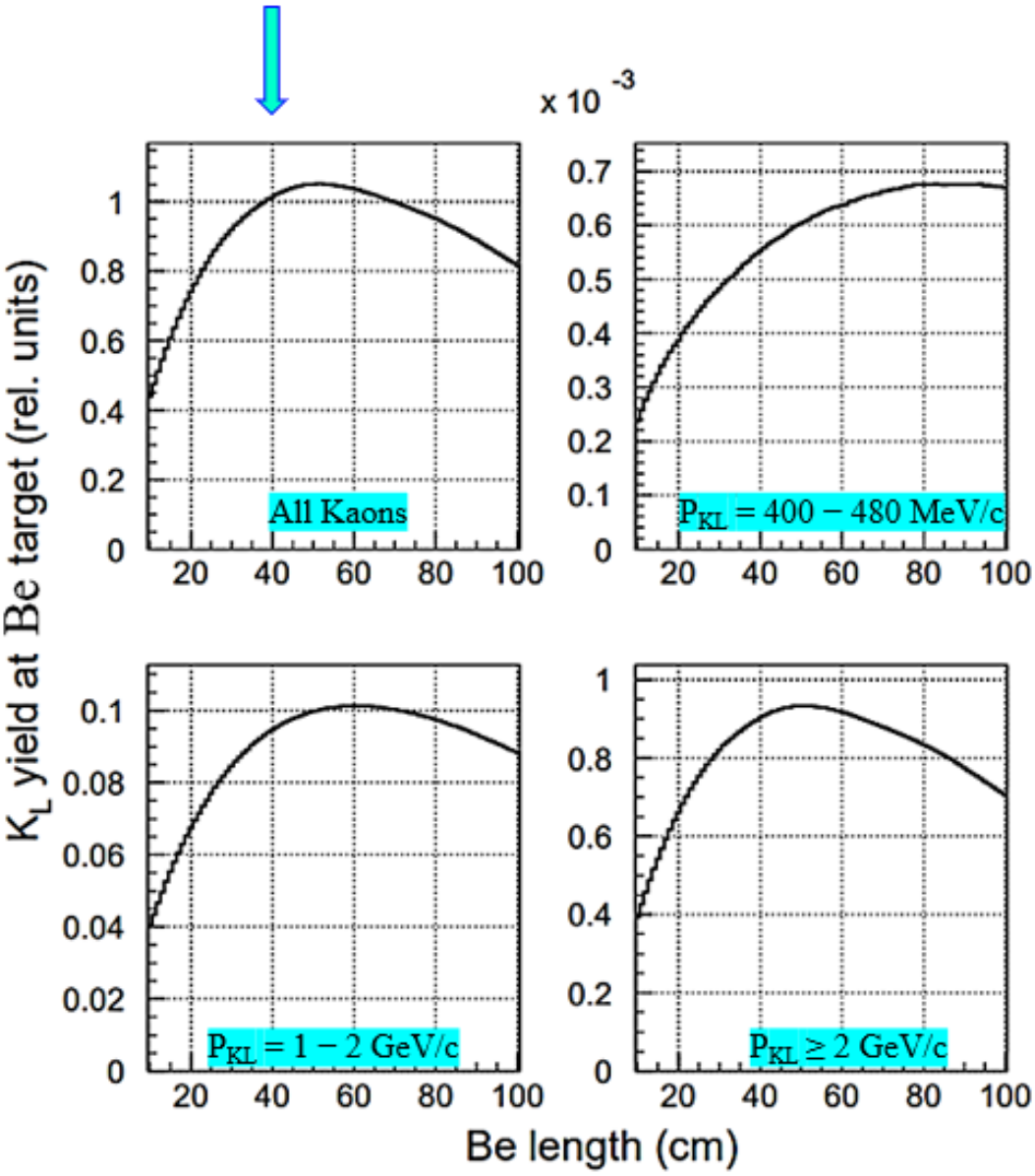

FIG. 6. Dependence of the K-long yield at the GlueX cryogenic LH_2 target on the thickness of the target for the different K_L momenta ranges. Top Left: For all K_L momenta, P_{KL} . Top Right: For $P_{KL} = 400 - 480$ MeV/c . Bottom Left: For $P_{KL} = 1 - 2$ GeV/c . Bottom Right: For $P_{KL} \geq 2$ GeV/c .

model of the KLF beamline. The MCNP model simulated a 12 GeV 5 μA electron beam hitting the copper radiator inside of the CPS. Electrons were transported through the copper radiator where they produced bremßtrahlung photons, which, in turn, were transported through the vacuum pipe until they hit the beryllium target. Secondary particles including neutrons and photons were traced in all components of the MCNP model. However, areas outside the concrete walls of the collimator alcove and the bremßtrahlung photon beam pipe were excluded from the model to increase the calculation speed. Additionally, we replaced the detailed models of the pair spectrometer and flux monitor magnets with five iron blocks placed around the beam pipe at the entrance of the main experimental hall that contains GlueX spectrometer.

Fig. 8 shows that our simulations for the KLF K_L and neutron flux (Fig. 8 (left)), which are qualitatively similar with the K_L spectrum measured by SLAC at 16 GeV [21] (Fig. 8 (right)). The KLF K_L flux is primarily over the range $p(K_L) = 1 - 10$ GeV/c, with a maximum flux near 4 GeV/c. The neutron flux falls sharply as the neutron

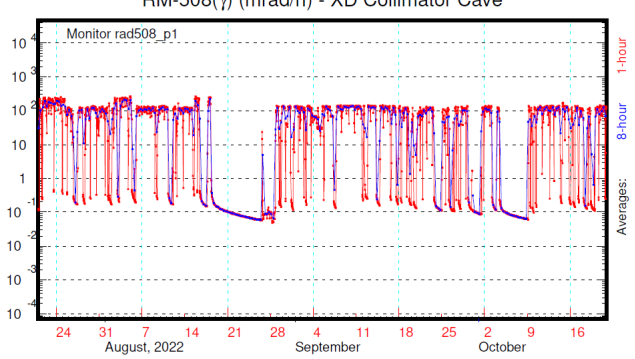

FIG. 7. A typical radiation environment in the Hall D Collimator Cave. Average hourly (red) and 8 h (blue) readings of the radiation monitors RM-508 are shown as a function of the calendar time during the Hall D operations in July-October of 2022.

momentum increases, and is mostly limited to $p(n) < 2$ GeV/c.

D. Neutron Flux on the Upstream Face of the GlueX Spectrometer

The neutron flux produced by the KPT has the potential to affect components of the GlueX spectrometer. The most sensitive components are the silicon photomultipliers (SiPMs) used for the Start Counter (SC) [23–25] and Barrel Electromagnetic Calorimeter (BCAL) [25, 26], which are located on the upstream end of the GlueX spectrometer. The SiPM detectors are only sensitive to neutron energies above 1 MeV [22]. To investigate the potential effect on these sensors, we calculated the prompt neutron dose rate for these neutron energies as a function of radial distance on the upstream end and show these results in Fig. 9 (left). The SiPMs used in the SC and BCAL are expected to tolerate this calculated neutron background. Previous studies state that the dose rate of 30 mrem/h increases the dark current at SiPM by a factor of 5 after 75 days of photon beam running [22]. The expected dose is well below this rate.

IV. RADIATION SAFETY REQUIREMENTS

In this section, we summarize the radiation safety requirements for the KPT and the calculations performed which show that these requirements are satisfied by the current KPT design. The task for the shielding design of the CPS in the Tagger enclosure and of the Beryllium target assembly in the Collimator Cave for the new experiment is to keep the radiation environment in their vicinity at or below the typical current level, both during and after the beam delivery. The radiation safety considerations are taken into account in the Beryllium target assembly design as explained in the Sections III.C and III.D above. The final design will be reviewed by the Radiation Physics Group at JLab for the final adjustments and approval when it is ready.

V. PROMPT DOSE

The prompt radiation dose in the KPT alcove affects the lifetime of materials and equipment. We calculate the prompt dose in the region of the KPT and the adjoining labyrinth using a FLUKA simulation. The layout of this region and corresponding map of prompt dose at the nominal beam current of 5 μA is shown in Fig. 10. These simulations show that most of the prompt radiation is contained in the KPT, and the rates outside the KPT meet the requirements of radiation safety at JLab which is 1 mrem/h [19].

As an additional check, we calculate the prompt radiation dose rate for neutrons (photons) in the experimental hall at the key area for RadCon on the ceiling using MCNP. We find a rate of 0.27 ± 0.08 mrem/h (0.065 ± 0.002 mrem/h), which is also under the limit of 1 mrem/h [19].

VI. ACTIVATION DOSE

The FLUKA model used for the activation calculations is more complicated. It includes the CPS, tagger hall, the beam line from the tagger hall to the KPT, and the KPT along with a more extensive model of the labyrinth and the rest of the collimator cave enclosure. The activation dose equivalent rates were calculated in units of pSv/s using the FLUKA code after 1000 hours of continuous operation at the electron beam current 5 μA. The corresponding equivalent dose rates after the end of beam delivery for 1 hour, 1 day, 1 week, and 1 month respectively are shown on Fig. 11 and summarized in Table I. According to this figure the activation level around the KPT after one hour is below the limit for high radiation area (100 mrem/h) and therefore meets the requirements of radiation safety at JLab.

The activation dose rate after 1000 h of operation in the KPT labyrinth is shown on Fig. 12. From this figure, we conclude that the dose rate near the exit from the KPT labyrinth to the main part of the experimental hall is below the JLab allowed limit of 1 mrem/h.

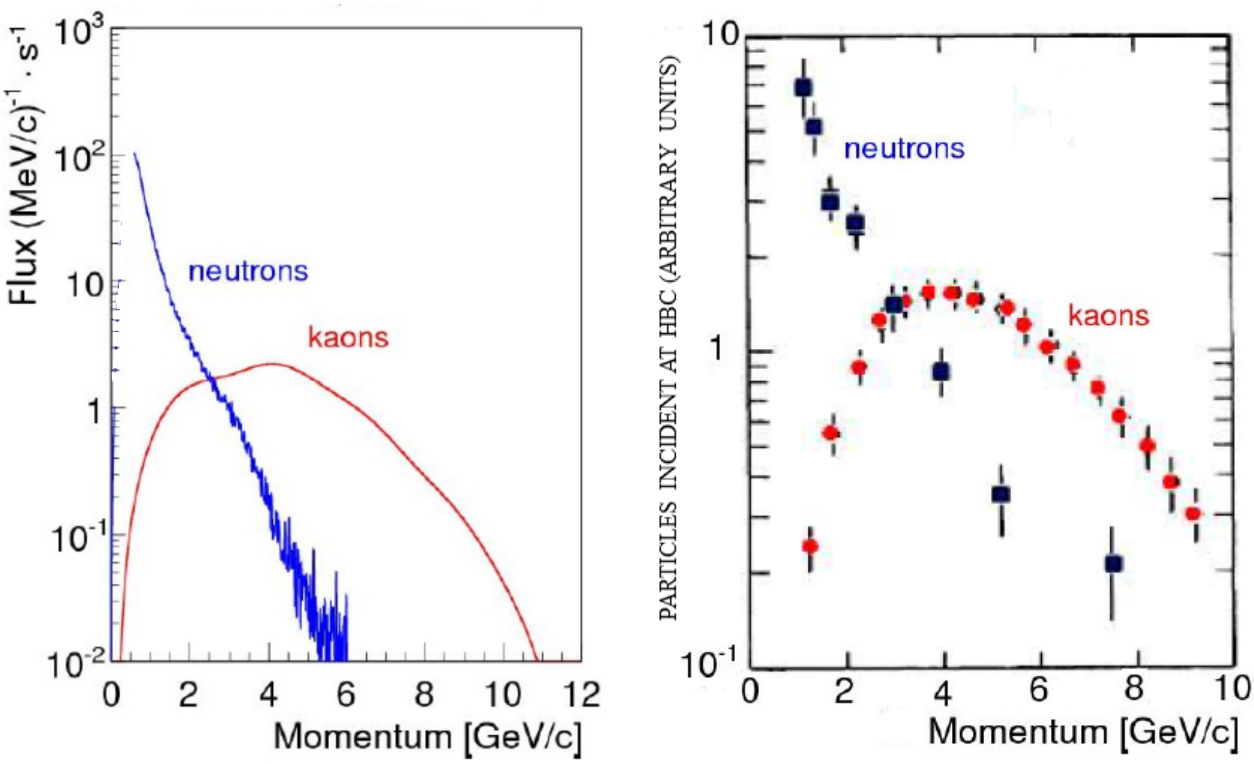

FIG. 8. The K_L and the neutron momentum spectra on the cryogenic target. Left: Rate of K_L (red) and neutrons (blue) on the LH_2/LD_2 cryogenic target of Hall D as a function of their generated momenta, with a total rate of $\sim 10^4$ K_L/sec and 6.6×10^5 n/sec, respectively. The K_L flux calculations were performed using Pythia generator [18] while the neutron flux calculations were performed using the MCNP transport code [12]. Right: Experimental data from SLAC measurements using a 16 GeV/c electron beam were taken from Ref. [21] (Figure 3).

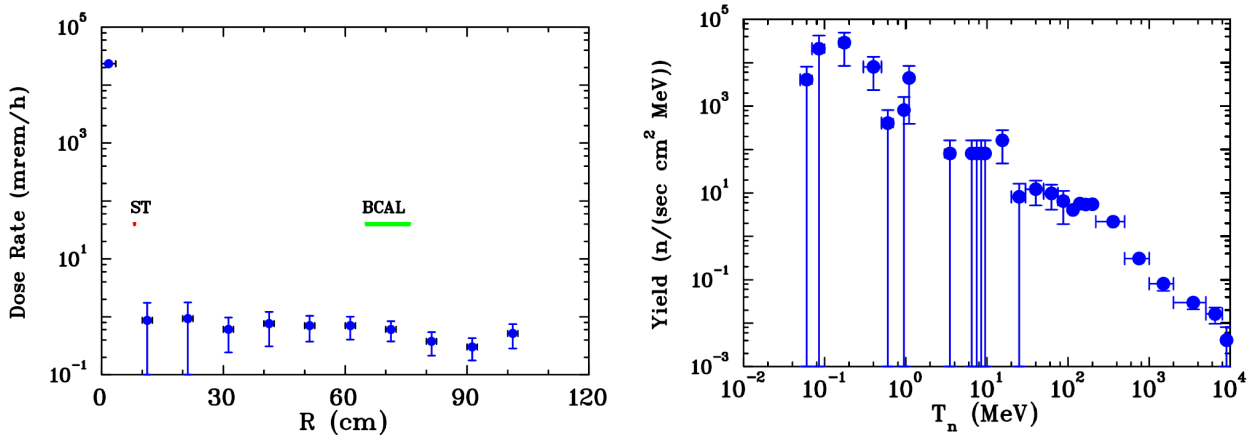

FIG. 9. Left: Prompt neutron radiation dose rate background calculated for SiPM of SC and BCAL on the face of the cryogenic target. In this case, we did not take into account additional shielding in the experimental hall. Right: Neutron energy spectrum in the beam on the face of the cryogenic target.

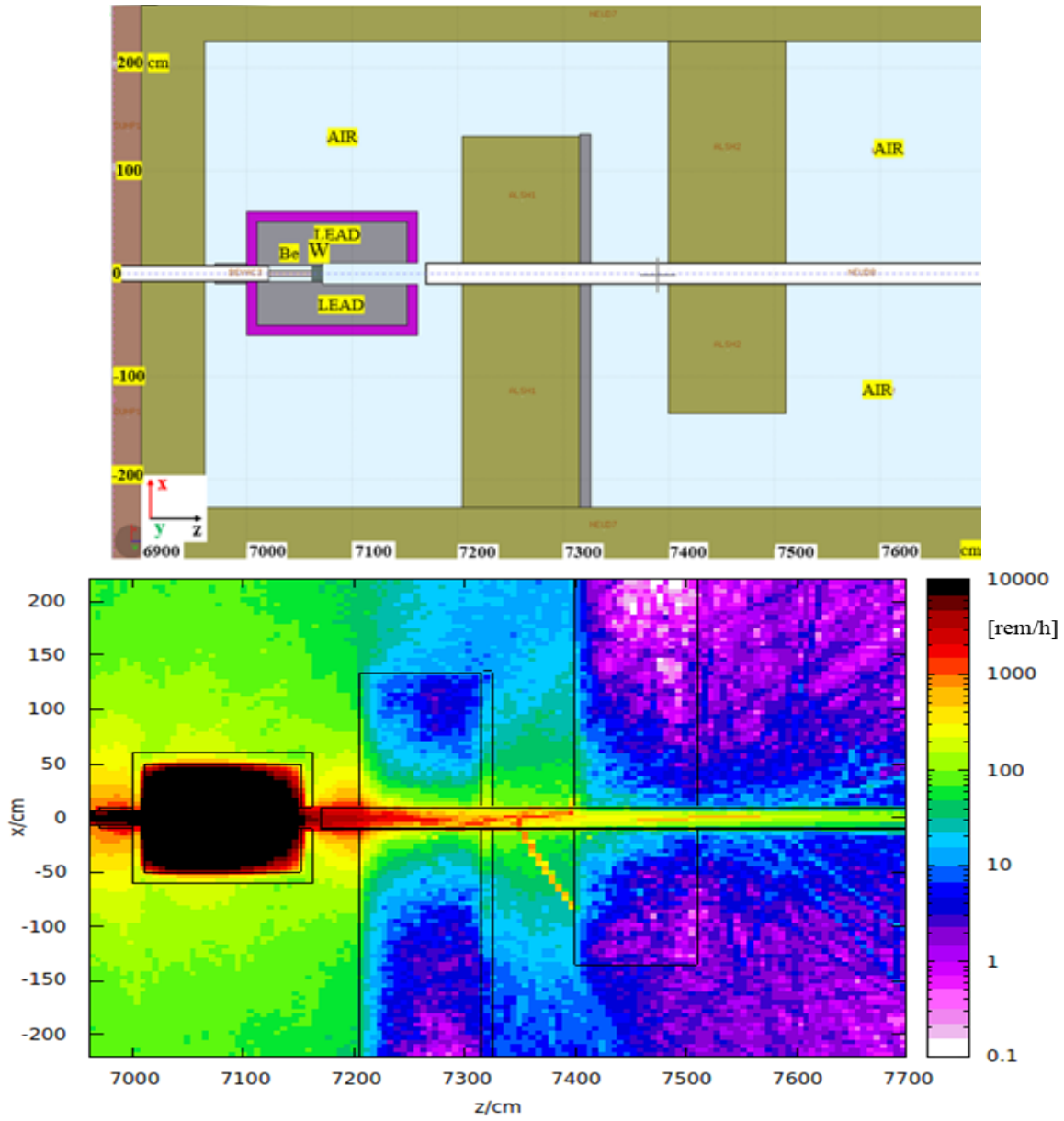

FIG. 10. Prompt dose equivalent in Collimator alcove. Top: – part of full CPS-KPT FLUKA model with KPT alcove. *brown* – soil, *khaki* – concrete, *blue* – air, *grey* – lead, *pink* – borated polyethylene. *green* – tungsten, *light pink* – beryllium. Bottom: – prompt dose equivalent map in rem/h at the electron beam current 5 μA. Horizontal scale – coordinate along the photon beam line in cm. Vertical scale – horizontal coordinate in cm. Color scale – prompt dose equivalent in rem/h within vertical coordinate $-150 < \mathrm{y/cm} < 150$ relative to the beam line. From these plots, we conclude that the equivalent dose level around the KPT meets the requirements of the radiation safety at JLab.

TABLE I. Activation estimates around KPT assembly at $\mathrm{r} = 90$ cm, 7000 cm $< \mathrm{z} < 7150$ cm .

Activation after one (units)	Hour	Day	Week	Month
pSv/s	3.5×10^4	2×10^4	0.5×10^3	1×10^2
mrem/h	13	8	0.2	0.04

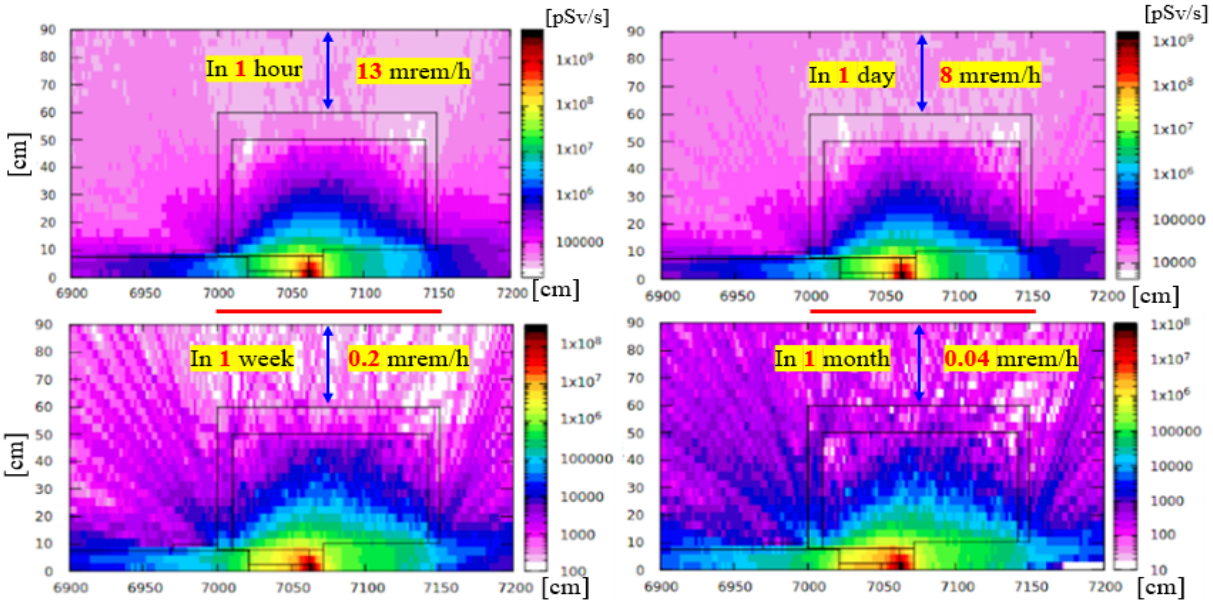

FIG. 11. Activation dose in materials of KPT and around it's surface after 1000 hours of continuous operation at electron beam current 5 μA and energy 12 GeV. Equivalent dose in pSV/s after 1 hour accelerator operational pause. Top Left: – After one hour. Top Right: – After one day. Bottom Left: – After one week. Bottom Right: – After one month. Horizontal scale – coordinate along the photon beam line in cm. Vertical scale – radial coordinate in cm. Color scale – equivalent dose in pSv/s. Equivalent dose 10^5 pSv/s = 36 mrem/h. The numerical estimates of activated dose at 30 cm distance form the KPT surface ($r/cm = 90, 7000 < z/cm < 7150$) are given in Table I. From these plots, we conclude that the activation level around the KPT meets the requirements of the radiation safety at JLab.

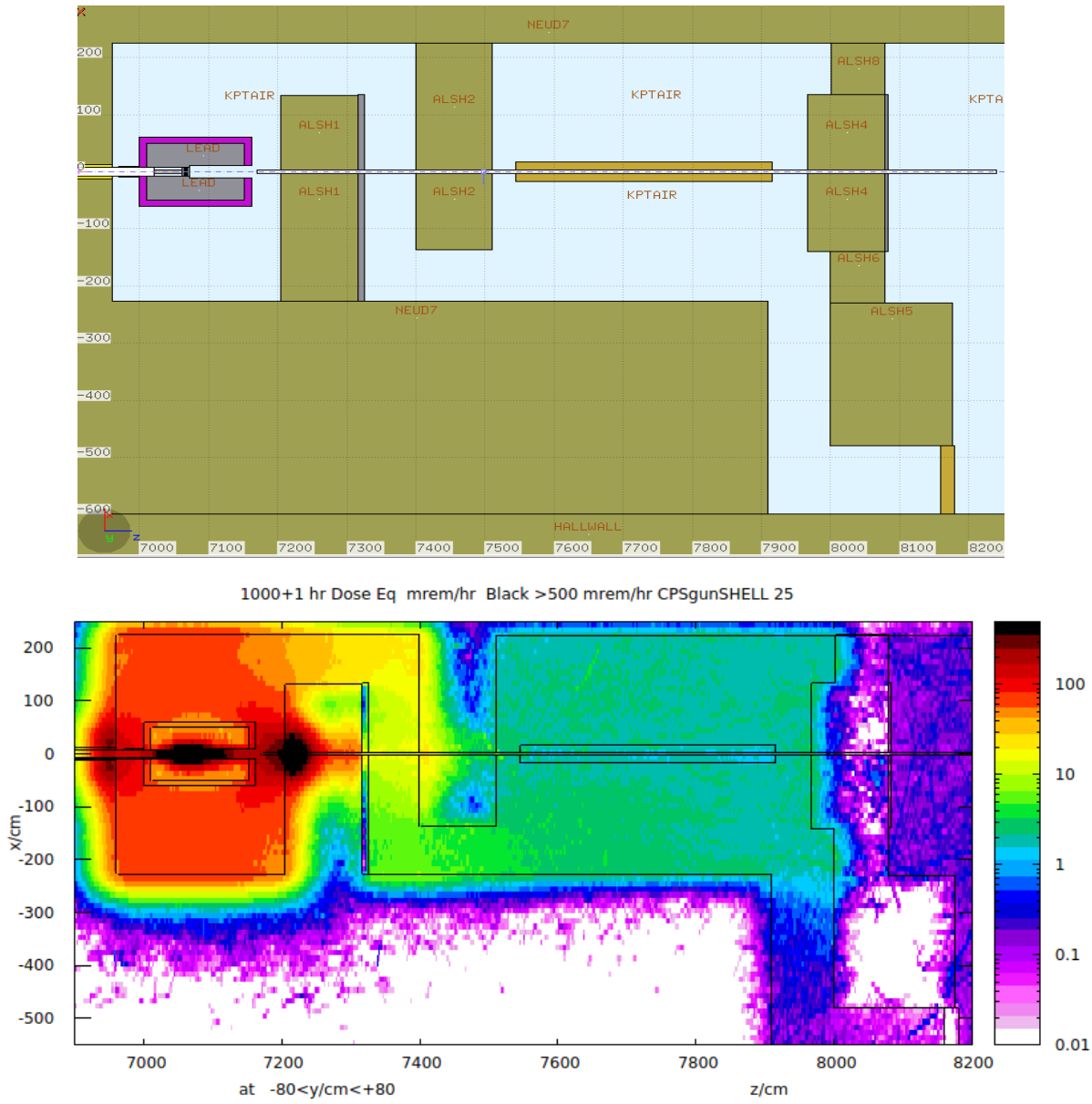

FIG. 12. Activation dose in KPT labyrinth after 1000 hours of continuous operation at electron beam current 5 μA and energy 12 GeV. Top: Plan view of the KPT labyrinth. Entry door is marked with red color. Vertical scale - in hall horizontal coordinate x in cm. Horizontal scale - in hall coordinate along beam z in cm. Bottom: Equivalent dose in mrem/hr after 1 hour accelerator operational pause. Horizontal scale – coordinate along the photon beam line in cm. Vertical scale – horizontal coordinate in cm. Color scale – equivalent dose in $mrem/hr$. Equivalent dose 10^5 pSv/s = 36 mrem/h. From these plots, we conclude that the activation level near the exit from KPT labyrinth meets the requirements of the radiation safety at JLab (below 1 mrem/hr).

VII. SIMULATION OF POWER DEPOSITION IN KPT

In this Section, we consider the power distribution in the KPT. We have calculated this distribution using a simplified model of the corresponding beamline using the FLUKA software [30].

A. Beam Line Model in FLUKA

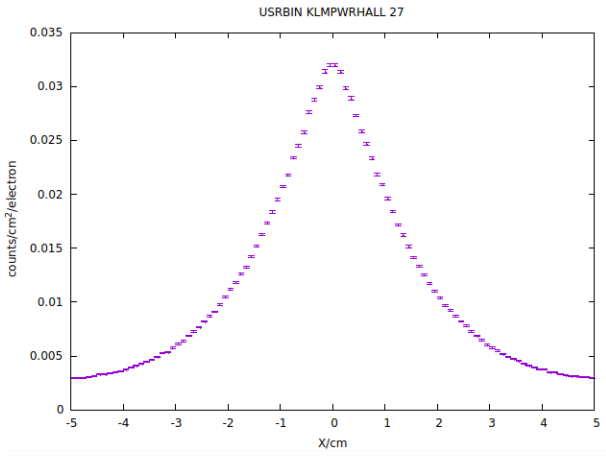

FIG. 13. Secondary photon beam profile at the entry of the Be target. Vertical scale - emission probability in a.u, horizontal scale - photon coordinate across the target in cm.

The simplified beamline model was developed with a goal to provide high rate of calculations. The 12 GeV electron beam hits the copper target 1.4 mm thick (10% of its radiation length). The photon beam propagates to a 67 m distance where it hits the beryllium target. The secondary photon beam is very well focused on the Be target 6 cm in diameter – the photon beam profile on the Beryllium target is shown in Fig. 13

B. Energy Deposition in the Kaon Production Target

The FLUKA model of the kaon production target assembly is shown in Fig. 14.

The energy deposition map inside the target is shown in Fig. 15. The color scale is given for the energy deposition in units of GeV/cm^3/electron. In order to estimate the power density in GeV/cm^3/s this value has to be scaled by the electron beam intensity of 3×10^{13} electrons/s at the nominal beam current 5 μA. In order to convert it to Watts/cm^3 an additional scale factor of 1.6×10^{-10} J/GeV is required. For example, the maximum energy deposition 0.01 GeV/cm^3/electron translates to 48 W/cm^3.

The effect of the tails of the photon beam that pass through the beam pipe is clearly seen in Fig. 15 at the entry to the KPT. This can also be seen by comparing the projection along the z-coordinate for the full KPT (Fig. 16), and for $R < 4$ cm, which consists mostly of the Be target and tungsten plug (Fig. 17). So, the photon beam tails create an additional source of radiation from the surface of the KPT.

We note that the spectrum of photons on the face of the Be-target generated using this simplified model by FLUKA agrees well (within ≈10%) with the detailed MCNP calculations for $E_\gamma > 0.2$ MeV and simple analytical models.

VIII. HEATING

The tungsten absorber block with dimensions of $(15.25 \times 15.25 \times 10)$ cm^3 will absorb most of the photon beam energy totaling over 5 KW in power. Therefore, it is necessary to cool the absorber with water to prevent any of the lead parts of the KPT assembly from melting. Figure 18 shows the water cooling setup for the tungsten plug which consists of four copper plates cooled with water at 35°C supply temperature. The copper tubes are soldered to the copper plate. The cooling system is designed to provide 2 gallons/min water flow through the tubes.

We performed a detailed study with steady-state thermal analysis using simulated data from the FLUKA model for the power absorption in the tungsten block described in the previous Section VII as the input for the calculations. The temperature calculations include the heat transfer through the homogeneous tungsten material towards the copper plates on the sides as well as the heat transfer from the copper to the cooling water flowing through the tubes.

Figure 19 shows the temperature distributions in the absorber versus x- and y-coordinates (left) at the depth of z = 2.5 cm inside the tungsten block, and the temperature versus r- and z-coordinates at the azimuthal angle of $\phi = 45^0$ (right). The cooling copper plates surrounding the tungsten plug are not shown in this Figure. Figure 20 shows the temperature dependence on the radial coordinate at the z = 2.5 cm depth and at azimuthal angle $\phi = 45^0$ (left), and the dependence on the z-coordinates at r = 0 cm and the azimuthal angle of $\phi = 45^0$ (right). The results show that the maximum temperature inside the tungsten plug will be at the depth of about z = 2.5 cm inside the tungsten block along the beam, and the value of the temperature at that point is expected to be 220°C with the described cooling configuration. The temperature at the sides of the tungsten plug at the depth of the maximum heat deposition z = 2.5 cm and in the horizontal plane on the beamline level is expected to be around 65°C. The temperature at the upstream face of the tungsten plug at the point of beam impact is expected to be around 180°C. Based on these results, we conclude that

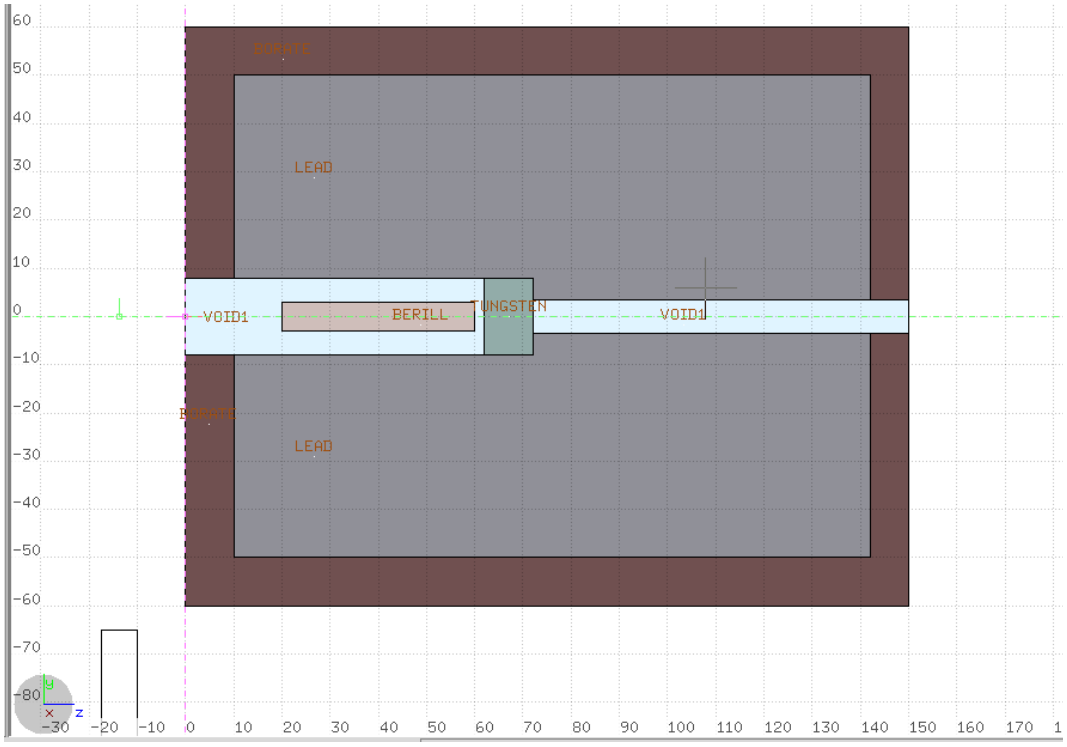

FIG. 14. The FLUKA model of the Kaon Production Target assembly. Vertical scale - R-coordinates, horizontal scale - coordinate along photon beam directions. Be "target" is a cylinder (light pink), 6 cm diameter and 40 cm long in a air filled pipe 8 cm in radius. The Be target length corresponds to 1.75 r.l. and was optimized at SLAC. It was shown that the further increase of the length of the target is not effective as it leads to the rapid falloff of K_L momentum spectrum [21]. Following the target is a "plug" of tungsten (light green) 8 cm radius and 10 cm thick, which is followed by an open pipe 5 cm radius; the Pb-shield is a cylinder (light blue) with sizes $R \times L = (50 \times 132)$ cm^2; the B-doped polyethylene layer (brawn) is sized as (60×150) cm^2. A "black wall" located at $z = -20$ cm with a hole of 3 cm by radius may be placed in front of the target to form a beam profile shown in Fig. 13(top).

.

the current design for the tungsten plug cooling system is sufficient to prevent any significant overheating of the material around the tungsten.

A. Beryllium Target Cooling

Since there is a concern with air contamination from the beryllium if air is blown onto the surface for cooling, it is decided to use water cooling for this target (Fig. 21). A maximum temperature of 66°C was found in the beryllium. The target is wrapped with a 0.065 inch thick copper sheet in which 0.25 inch cooling tubes are brazed on to. The inner surface of the water cooling tube is assumed to have a convection coefficient of $5,000$ W/m^2 K and a water temperature of 40°C on average. Hand calculations and ANSYS steady state thermal calculations [32] are in close agreement. The model takes into consideration imperfect thermal contact between the beryllium and copper cooling sheet by incorporating a 100 μ air gap between the 2 surfaces. This is very conservative since there will be some actual contact. 300 W is applied to a theoretical 1 mm diameter hole over the entire length of the cylindrical surface.

IX. SUMMARY

In this document, we have described a conceptual design for a Kaon Production Target that satisfies the requirements of the KLF project as well as the physical and radiological requirements of Jefferson Lab.

Simulations were performed to optimize the dimensions of the target and various shielding configurations with a goal to maximize the flux of K$_L$'s keeping neutron and gamma radiation at the level limited by the safety requirements at Jefferson Lab. The resulting kaon flux is $\sim 10^4$ K$_L$/sec, which meets the requirements for the KLF project, while the neutron and gamma fluxes and corresponding prompt dose rates are safely below the radiation dose rate limits established by the Radiology Control Division of Jefferson Lab.

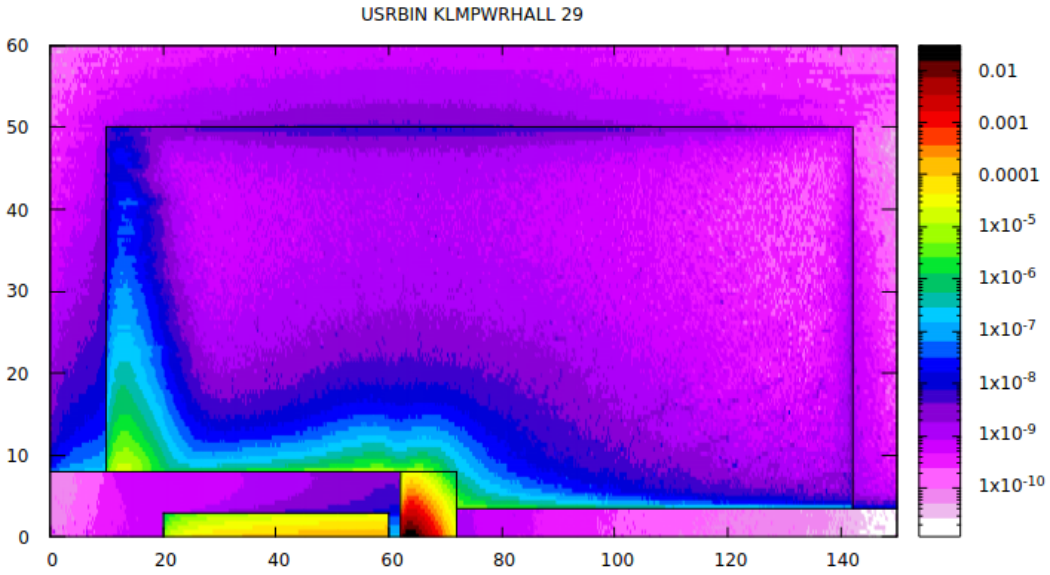

FIG. 15. Energy deposition inside the borated shielding cylinder of the KLF KPT. Vertical scale – radial coordinate in cm, horizontal scale – Z-coordinate along the photon beam in cm. Color scale – energy deposition in GeV/cm^3/e.

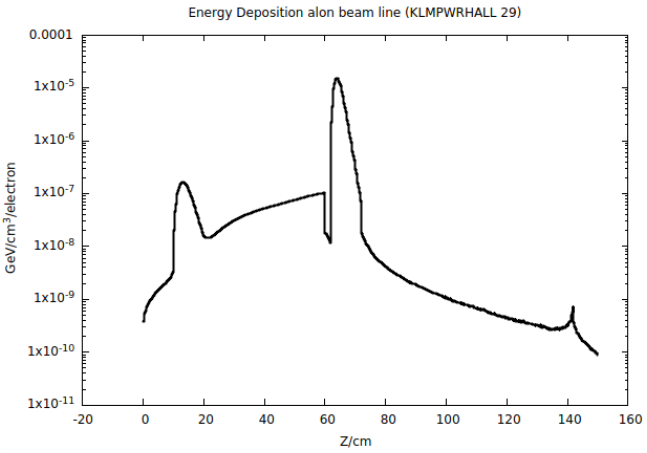

FIG. 16. Power distribution in KPT target along its z-coordinate.

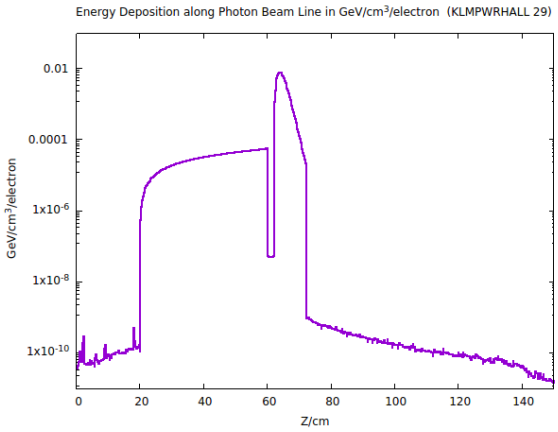

FIG. 17. Power distribution along Z-axis for $R < 4$ cm, *i.e.*, in the cylinders of the Be target and tungsten plug.

Since significant beam power is deposited in the central part of the KPT, special attention was devoted studying the heat distribution inside KPT. The temperature map inside KPT was obtained using the ANSYS software package using the energy deposition map from the FLUKA as an input, and no overheating elements were found.

X. ACKNOWLEDGMENTS

We are thankful to Stephanie Worthington for details of the geometry of the collimator alcove. This work was supported in part by the U. S. Department of Energy, Office of Science, Office of Nuclear Physics under Awards Nos. DE–SC0016583, DE–FG02–96ER40960, DE–AC05–06OR23177, and DE–FG02–92ER40735, and also by the U. K. STFC ST/L00478X/1 and ST/P004008/1 grants.

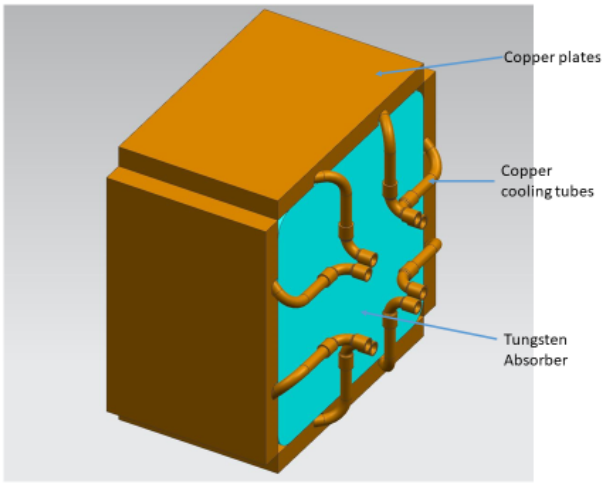

FIG. 18. Tungsten absorber cooling setup. The teal color rectangular block represents the tungsten absorbed while the copper cooling system is represented with golden brown color.

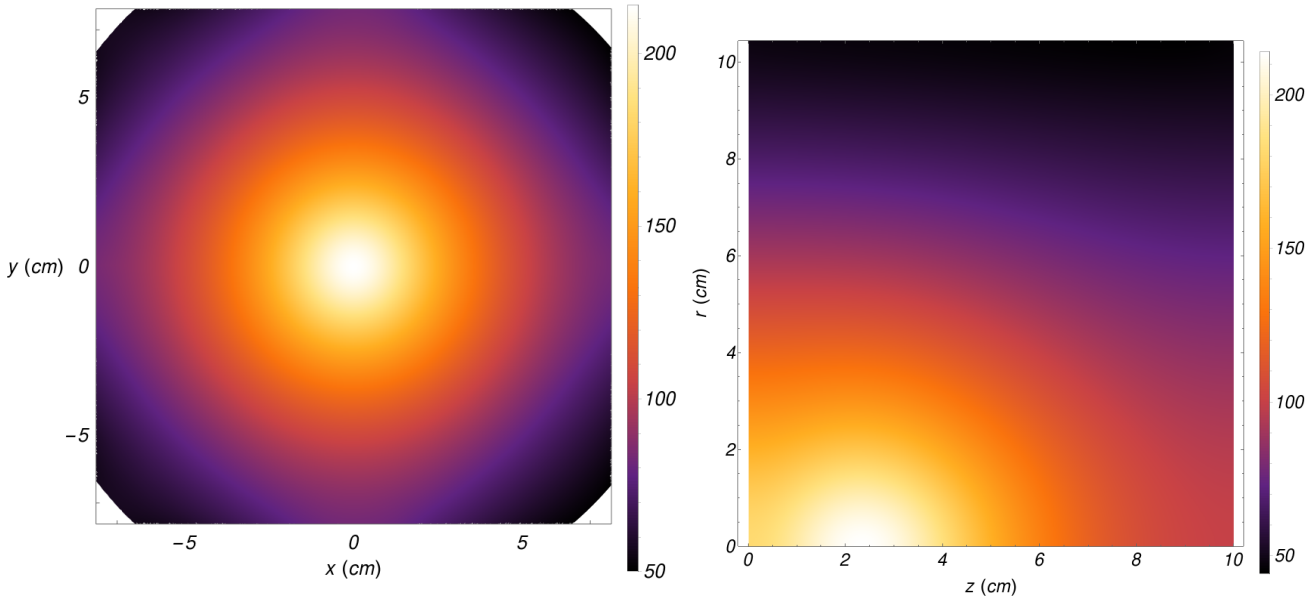

FIG. 19. Temperature distribution inside the tungsten absorber versus x- and y-coordinates at the depth of z = 2.5 cm along the beam direction inside the tungsten block (left), and temperature versus radial and axial coordinates at an azimuthal angle of $\phi = 45^0$ (right).

[1] *Strange hadron spectroscopy with secondary K_L beam in Hall D*, Spokespersons: M. J. Amaryan, M. Bashkanov, S. Dobbs , J. Ritman, J. R. Stevens, and I. I. Strakovsky (KLF Collaboration), JLab C2–12–19–001, Newport News, VA, USA, 2019; [arXiv:2008.08215 [nucl-ex]].

[2] S. Adhikari *et al.* [GlueX Collaboration], "The GLUEX beamline and detector," Nucl. Instrum. Meth. A **987**, 164807 (2021).

[3] A. Aprahamian *et al.*, *Reaching for the horizon: The 2015 long range plan for nuclear science*; http://science.energy.gov/np/nsac/ .

[4] PAC48 Final Report, https://www.jlab.org/exp_prog/PACpage/PAC48/PAC48_PrelimReportPlus_FINAL.pdf .

[5] D. Day *et al.*, "A conceptual design study of a Compact Photon Source (CPS) for Jefferson Lab," Nucl. Instrum.

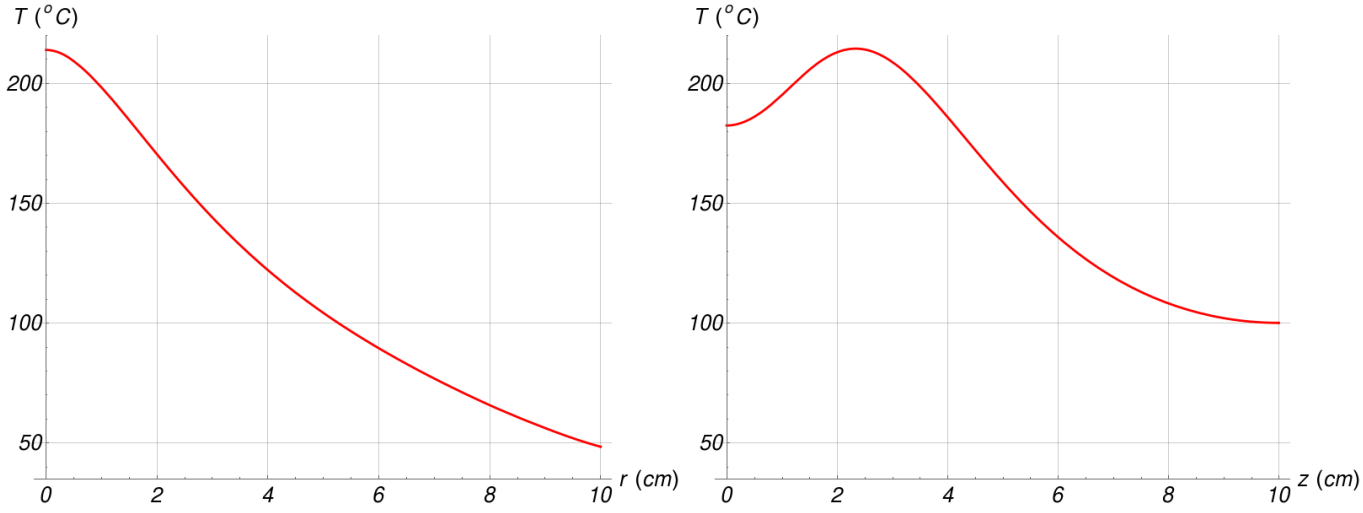

FIG. 20. Temperature inside the tungsten absorber versus radial coordinate r at the z = 2.5 cm depth and $\phi = 45^0$ azimuthal angle (left), and temperature versus z along the beamline at r = 0 cm and the azimuthal angle of $\phi = 45^0$ (right).

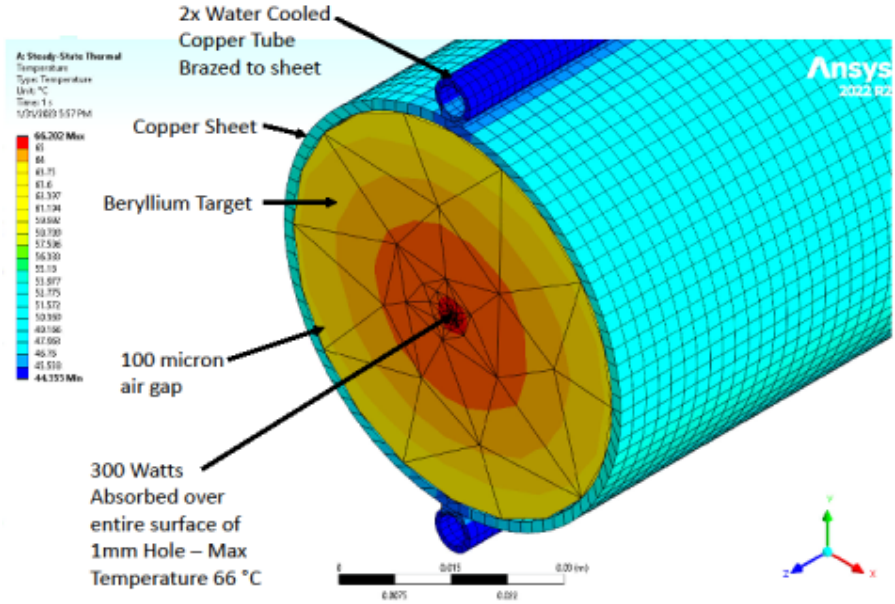

FIG. 21. Water cooled Beryllium target ANSYS results.

Methods, A **957**, 163429 (2020).

[6] V. Baturin, M. Amaryan, E. Chudakov, P. Degtyarenko, S. Dobbs, H. Egiyan, C. E. Hyde, I. Strakovsky, and T. Whitlatch, "The Compact Photon Source for Hall D at Jefferson Laboratory (Technical Note)," in progress.

[7] M. Bashkanov, D. P. Watts, N. Zachariou, E. Chudakov, M. Amaryan, J. Ritman, J. Stevens, and I. Strakovsky, "KL flux monitor," Preprint GlueX-doc-3603, 2019.

[8] R. Yamartino *et al.*, "A study of the reactions $\bar{K}^0 p \to \Lambda\pi^+$ and $\bar{K}^0 p \to \Sigma^0\pi^+$ from 1-GeV/c to 12-GeV/c," Phys. Rev. D **10**, 9 (1974); R. Yamartino, "A study of the reactions $\bar{K}^0 p \to \Lambda\pi^+$ and $\bar{K}^0 p \to \Sigma^0\pi^+$ from 1-GeV/c to 12-GeV/c," SLAC-R-0177, SLAC-R-177, SLAC-0177, SLAC-177.

[9] S. Adhikari *et al.* [GlueX Collaboration], "Beam asymmetry $\mathbf{\Sigma}$ for the photoproduction of η and η' mesons at $E_\gamma = 8.8$ GeV," Phys. Rev. C **100**, 052201 (2019).

[10] A. Ali *et al.* [GlueX Collaboration], "First measurement of near-threshold J/ψ exclusive photoproduction off the proton," Phys. Rev. Lett. **123**, 072001 (2019).

[11] H. Al Ghoul *et al.* [GlueX Collaboration], "Measurement of the beam asymmetry Σ for π^0 and η photoproduction on the proton at $E_\gamma = 9$ GeV," Phys. Rev. C **95**, 042201 (2017)

[12] T. Goorley *et al.*, "Initial MCNP6 release overview," Nucl. Tech. **180**, 298. (2012); https://mcnp.lanl.gov/ .

[13] A. D. Brody *et al.*, "Production of K0(2) mesons and neutrons by 10-GeV and 16-GeV electrons on beryllium," Phys. Rev. Lett. **22**, 966 (1969).
[14] M. G. Albrow *et al.*, "Photoproduction of K^0 mesons from protons and from complex nuclei," Nucl. Phys. B **23**, 509 (1970).
[15] N. Petoussi-Henss, W. E. Bolch, K. F. Eckerman, A. Endo, N. Hertel, J. Hunt, M. Pelliccioni, H. Schlattl, and M. Zankl, *ICRP, 2010. Conversion Coefficients for Radiological Protection Quantities for External Radiation Exposures*, ICRP 116 Publication, Editor C. H. Clement, Ann. ICRP, **40**, (2-5) (2010).
[16] R. G. Williams III, C. J. Gesh, and R. T. Pagh, *Compendium of material composition data for radiation transport modeling*, PNNL–15870, 2006.
[17] G. Battistoni, T. Boehlen, F. Cerutti, P. W. Chin, L. S. Esposito, A. Fassò, A. Ferrari, A. Lechner, A. Empl, A. Mairani *et al.* "Overview of the FLUKA code," Annals Nucl. Energy **82**, 10 (2015); version FLUKA2021.2.9.
[18] We used a modified version of the Pythia [20] package for the GlueX Collaboration at JLab Hall D, http://home.thep.lu.se/torbjorn/Pythia.html .
[19] Pavel Degterenko, private communication.
[20] T. Sjöstrand *et al.*, "An introduction to PYTHIA 8.2," Comput. Phys. Commun. **191**, 159 (2015).
[21] G. W. Brandenburg *et al.*, "Production of K0(l) mesons and neutrons from electrons on beryllium above 10-GeV," Phys. Rev. D **7**, 708 (1973).
[22] A. Somov, "Neutron background estimates in the Tagger hall," Preprint GlueX–doc–1646, 2011.
[23] Y. Qiang, C. Zorn, F. Barbosa, and E. Smith, "Radiation hardness tests of SiPMs for the JLab Hall D Barrel Calorimeter," Nucl. Instrum. Meth. A **698**, 234 (2013).
[24] E. Pooser *et al.*, "The GlueX start counter detector," Nucl. Instrum. Meth. A **927**, 330 (2019).
[25] P. Degtiarenko, A. Fass, G. Kharashvili, and A. Somov, "Calculation of radiation damage to silicon photomultipliers in GlueX experiment," Preprint JLAB-TN-11-005, 2011.
[26] T. D. Beattie *et al.*, "Construction and performance of the Barrel Electromagnetic Calorimeter for the GlueX experiment," Nucl. Instrum. Meth. A **896**, 24 (2018).
[27] L. Keller, private communication, 2015.
[28] J. Allison *et al.*, "Recent developments in Geant4," Nucl. Instrum. Meth. A **835**, 186 (2016).
[29] I. Larin, "Simulation study of KL beam: KL rates and background," in: *Workshop on Physics with Neutral Kaon Beam at JLab*, mini-Proceedings, arXiv:1604.02141 [hep—ph] (February, 2016), p. 198.
[30] T. T. Böhlen, F. Cerutti, M. P. W. Chin, A. Fassò, A. Ferrari, P. G. Ortega, A. Mairani, P. R. Sala, G. Smirnov, and V. Vlachoudis, "The FLUKA code: Developments and challenges for high energy and medical applications," Nucl. Data Sheets **120**, 211 (2014).
[31] R. L. Workman [Particle Data Group], "Review of Particle Physics," PTEP **2022**, 083C01 (2022).
[32] ANSYS inc. Workbench 2022 R2 Finite Element Program.
[33] I. Strakovsky, M. Amaryan, M. Bashkanov, W. J. Briscoe, E. Chudakov, P. Degtyarenko, S. Dobbs, A. Laptev, I. Larin, A. Somov *et al.* "Conceptual design of beryllium target for the KLF project," [arXiv:2002.04442 [physics.ins-det]].

Appendix A: KPT Shield Layers and Weight

The approximation for the KPT weight (about $15,500$ kg) and components for the Collimator cave breakdown is given in Table II.

TABLE II. Cost estimates for the K-long Collimator Cave and its main parts by Timothy Whitlatch. One need to add about \$1K for cooling system for the beryllium. Total weight of the Be-target assembly is about $15,500$ kg.

Equipment	Qty	Cost each ($)	Fab cost ($)	Total Cost ($)
Beryllium target	1	11,000		11,000
Beryllium support	1	1,100		1,100
Tungsten absorber	1	12,000		12,000
Target lead bricks	1,190	52	2,000	63,800
Target Support structure	1	0	9,000	9,000
Hilman rollers	4	850		3,400
Rails	2		1,850	1,850
Wedge levelers	4	700		2,800
Leveler base plate	4		2,100	2,100
Borated poly sheets	24	800	4,800	24,000
Central support tubes	2	800		1,600
Hardware	76	2.5		190
Cooling plates	4	1,240		4,960
Water cooling system	1	20,000		20,000
Shielding wall lead bricks	792	52		41,184
Vacuum beamline	1	5,000		5,000
Concrete block shielding wall	1,188	6		7,128
Water cooling for beryllium	1	1,000		1,000
Active collimator stand	1	10,000		10,000
PLC	1	2,000		2,000
Temperature sensors and PLC comp	6	150		900
Support for shield wall	2	3,300		6,600
Total cost				231,692